Synthesis of Ethylene Hydridotris(1-pyrazolyl)borate Triphenylphosphine Complexes of Rhodium and Iridium and Their Reactions with Hydrogen

Warren J. Oldham, Jr., and D. M. Heinekey*

Department of Chemistry, University of Washington, Box 351700, Seattle, Washington 98195-1700

Received June 27, 1996[⊗]

Solutions of $TpM(C_2H_4)_2$ (M = Rh (**1a**) and Ir (**1b**)) react with 1 equiv of PPh_3 to yield $TpM(PPh_3)(C_2H_4)$ (**2a**,**b**). The new complexes adopt trigonal-bipyramidal structures in solution with triphenylphosphine coordinated in the axial site and ethylene positioned in the equatorial plane. For **2a** the axial and equatorial pyrazolyl arms of the Tp ligand exchange positions on the NMR time scale ($\Delta G^{\ddagger}$ = 14.3 kcal mol^{-1}, 279 K); however, no exchange is observed in the case of **2b**, even at 353 K ($\Delta G^{\ddagger}$ > 18.4 kcal mol^{-1}). Complexes **2a**,**b** react with molecular hydrogen to yield $TpM(PPh_3)H_2$ (**3a**,**b**) and free *ethylene*. Kinetic studies of the iridium system show that this reaction is first order in both **2b** and H_2 and is not inhibited by a 10-fold excess of ethylene or PPh_3 ($k_{H_2}/k_{D_2} = 1.26 \pm 0.18$). These results indicate that the H_2 addition reaction proceeds by rapid reversible dissociation of a pyrazolyl arm, through a square-planar (η^2-Tp)Ir(PPh_3)(C_2H_4) intermediate.

The hydridotris(1-pyrazolyl)borate (Tp) class of ligands generally forms stable metal complexes containing either a bidentate or tridentate array of nitrogen-ligated pyrazolyl arms:[1]

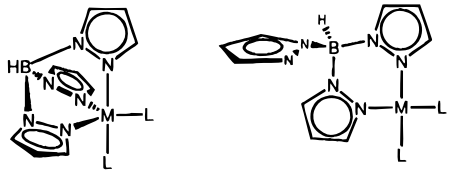

The subtle interplay between steric and electronic factors which favors one structure over another is clearly evident in the series of low-valent rhodium and iridium complexes of the form $Tp^{R2}ML_2$ (L = CO, CNR, olefin).[2−9] The solution-phase, ground-state coordination geometry in these species has been shown to be either trigonal bipyramidal (tbp) or square planar (sp) or a mixture of both, depending on the metal center, the substituents of the Tp ligand, and the donor ligands. The tbp structure is related to the sp form by simple dissociation of an equatorial pyrazolyl arm. Since little additional ligand rearrangement is required, this dynamic process is often observed with only small activation barriers. In fact, a dynamic equilibrium between tbp and sp structures has recently been carefully examined by Venanzi and co-workers for an extensive series of rhodium complexes, $Tp^{3R,4R,5R}Rh(LL)$ (LL = 2CO, norbornadiene (NBD), cyclooctadiene (COD)).[9,10] Solution-phase IR spectroscopy of the bis-CO complexes showed that, in certain cases, both tbp and sp forms were present in solution. By altering the substituents of the Tp ligand and/or the solvent, it was possible to shift the equilibrium to favor either five-coordinate tbp complexes or four-coordinate sp complexes. Similar isomeric mixtures have been observed by Trofimenko and coworkers in more elaborately substituted $Tp^{3R,4R,5R}Rh(CO)_2$ complexes.[11] In most cases the solution-phase structure mirrors that determined in the solid state by single-crystal X-ray diffraction. However, small crystal packing forces can favor selective crystallization of the minor isomer, thereby providing evidence for its existence in solution.[12] The ground-state structure of $TpM(C_2H_4)_2$ (M = Rh (**1a**),[13] Ir (**1b**)[14,15]) is not known with certainty. A static sp or tbp structure is expected to show a 2:1 pattern of pyrazolyl resonances by ^1H or ^{13}C NMR analysis. Instead, a fluxional process renders the pyrazolyl arms equivalent at all accessible temperatures. A tbp structure is suggested by low-temperature ^1H NMR studies of tetrakis(pyrazolyl)-borate analogs $(B(pz)_4)Rh(LL)$, which reveal two pyrazolyl environments in a 3:1 ratio when LL = COD,

[⊗] Abstract published in *Advance ACS Abstracts,* January 15, 1997.

(1) Substitution of the Tp ligand is represented by superscripts as suggested by Trofimenko. If the substituted position is not specified, then the priority is 3 > 5 > 4. For example, methyl substituents in the 3,5-positions are indicated as Tp^{Me2}. For a comprehensive review of this class of complexes see: Trofimenko, S. *Chem. Rev.* **1993**, *93*, 943−980.

(2) O'Sullivan, D. J.; Lalor, F. J. *J. Organometal. Chem.* **1974**, *65*, C47−C49.

(3) Cocivera, M.; Desmond, T. J.; Ferguson, G.; Kaitner, B.; Lalor, F. J.; O'Sullivan, D. J. *Organometallics* **1982**, *1*, 1125−1132.

(4) Cocivera, M.; Ferguson, G.; Lalor, F. J.; Szczecinski, P. *Organometallics* **1982**, *1*, 1139−1142.

(5) Ghosh, C. K.; Rodgers, D. P. S.; Graham, W. A. G. *J. Chem. Soc., Chem. Commun.* **1988**, 1511−1512.

(6) Ball, R. G.; Ghosh, C. K.; Hoyano, J. K.; McMaster, A. D.; Graham, W. A. G. *J. Chem. Soc., Chem. Commun.* **1989**, 341−342.

(7) Jones, W. D.; Hessell, E. T. *Inorg. Chem.* **1991**, *30*, 778−783.

(8) Ciriano, M. A.; Fernández, M. J.; Modrego, J.; Rodríguez, M. J.; Oro, L. A. *J. Organomet. Chem.* **1993**, *443*, 249−252.

(9) Bucher, U. E.; Currao, A.; Nesper, R.; Rüegger, H.; Venanzi, L. M.; Younger, E. *Inorg. Chem.* **1995**, *34*, 66−74.

(10) Bucher, U. E.; Fässler, T. F.; Hunziker, M.; Nesper, R.; Rüegger, H.; Venanzi, L. M. *Gazz. Chim. Ital.* **1995**, *125*, 181−188.

(11) Rheingold, A. L.; Ostrander, R. L.; Haggerty, B. S.; Trofimenko, S. *Inorg. Chem.* **1994**, *33*, 3666−3676.

(12) Cocivera, M.; Ferguson, G.; Kaitner, B.; Lalor, F. J.; O'Sullivan, D. J.; Parvez, M.; Ruhl, B. *Organometallics* **1982**, *1*, 1132−1139.

(13) Trofimenko, S. *J. Am. Chem. Soc.* **1969**, *91*, 588−595.

(14) Tanke, R. S.; Crabtree, R. H. *Inorg. Chem.* **1989**, *28*, 3444−3447.

(15) Fernández, M. J.; Rodriguez, M. J.; Oro, L. A.; Lahoz, F. J. *J. Chem. Soc., Dalton Trans.* **1989**, 2073−2079.

S0276-7333(96)00514-6 CCC: $14.00

duroquinone.[4] These are assigned to the dynamically averaged pyrazolyl ligands coordinated to the metal center and to the uncoordinated pyrazolyl arm, respectively. Likewise, a tbp structure was assigned to TpRh(COD) on the basis of a comparison of its ^{103}Rh NMR chemical shift to a number of related complexes.[9] Square-planar structures have been shown to be thermally accessible, indicated by exchange of free and bound pyrazolyl groups in $(B(pz)_4)M(LL)$ complexes (eq 1).[3,4,16] Even when this exchange is slow on the NMR

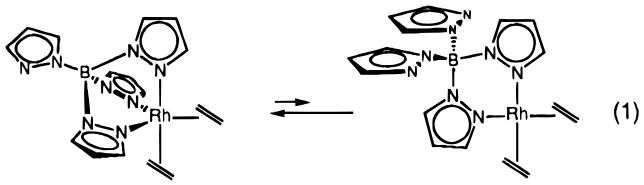
(1)

time scale, separate resonances for the sp form were not detected. We estimate that K_{eq} for equilibria of the type shown in eq 1 must therefore be less than 0.05 ($\Delta G° >$ 1.8 kcal mol^{-1}). Square-planar complexes derived from a similar equilibrium for **1a** and **1b** should provide a low-energy pathway for substitution reactions.[17,18] For example, **1a** and **1b** are found to react rapidly with CO to give $[TpRh]_2(\mu\text{-}CO)_3$[2,3] and $TpIr(CO)_2$,[14] respectively. Influenced by these observations, we felt that **1** might be an appropriate starting material to prepare a variety of phosphine-substituted complexes based on the $TpM(PR_3)$ fragment. Indeed, **1a** and **1b** react cleanly with PPh_3 to give $TpM(PPh_3)(C_2H_4)$ (**2a**,**b**). This paper details the synthesis, solution-state structure and dynamics, and hydrogen addition reactions of **2a**,**b**. Solutions of **2a** and **2b** react with H_2 to yield $TpM(PPh_3)H_2$ (**3a**,**b**) and free *ethylene*. Although the ground-state structure of **2** is found to be tbp, kinetic evidence is presented which indicates that sp, η^2-Tp complexes are important intermediates in the formation of **3**.

Results

Synthesis and Solution-State Structure of TpM(PPh$_3$)(C$_2$H$_4$). Solutions of **1a** or **1b** react at the time of mixing with PPh_3 to yield **2a** or **2b**, respectively (eq 2). Reactions conducted in sealed NMR tubes (stored

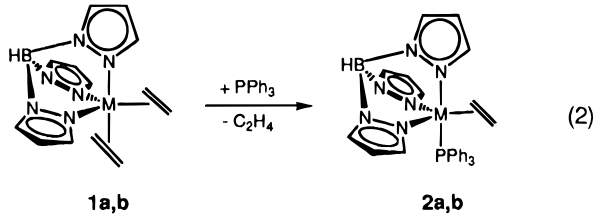

(2)

1a,b **2a,b**

at 77 K and then warmed to 195 K immediately before use) and monitored by ^{1}H NMR spectroscopy at low temperature (200 K) were complete in less time than it was possible to acquire an NMR spectrum (<2 min). Separate experiments carried out in the same fashion except for addition of excess ethylene to each NMR tube gave identical results. Solutions of **2a** or **2b** protected from air and light are stable at room temperature for weeks in common solvents, although **2a** rapidly decomposes in chlorinated solvents. **1a** was previously reported to decompose to a mixture of uncharacterized products upon reaction with PPh_3 in CH_2Cl_2.[2,3] We find that reaction in any non-halogenated solvent such as THF, benzene, or toluene results in clean and quantitative conversion to **2a**. Concentration of these solutions and addition of pentane affords yellow or very pale yellow microcrystalline samples of **2a** and **2b**, respectively. Carmona and co-workers have also recently reported that $Tp^{Me2}Rh(C_2H_4)_2$ reacts at 20 °C with CO, PMe_3, or tBuNC to yield stable $Tp^{Me2}Rh(L)(C_2H_4)$ complexes in benzene.[19] $Tp^{Me2}Ir(C_2H_4)_2$ reacts at 60 °C in neat thiophene to yield $Tp^{Me2}Ir(SC_4H_4)(2\text{-thienyl})_2$.[20]

Variable-temperature ^{1}H and ^{13}C{^{1}H} NMR and selected NOE experiments have been undertaken to establish the solution-state structures of **2a** and **2b**. These data indicate that a common tbp geometry is obtained in solution with PPh_3 coordinated in the axial site and ethylene positioned in the equatorial plane. Broad, ill-defined resonances for the Tp and PPh_3 ligands are observed at room temperature in the ^{1}H NMR spectrum of **2a**. Exchange of axial and equatorial pyrazolyl ligands and rotation about the Rh−P bond in the intermediate exchange region accounts for these broad lines. Dissociation of the PPh_3 ligand from the metal center was ruled out as a possible explanation for the broad aromatic resonances, since addition of excess PPh_3 yields identical line shapes attributed to the metal complex and sharp multiplets for free PPh_3. When the temperature is lowered, the Tp resonances decoalesce and sharpen into a 2:1 pattern characteristic of C_s symmetry. Analysis of the temperature dependence of the exchange between axial and equatoral pyrazolyl ligands using the method of Shanan-Atidi and Bar-Eli[21] gives an activation barrier for this process of 14.3 kcal mol^{-1} at the coalescence temperature of 279 K. Sharp resonances for the PPh_3 ligand are observed below 230 K, indicating slow rotation about the Rh−P bond. Hindered rotation about the Ir−P bond in the intermediate exchange region is also observed for **2b**, although no evidence for axial/equatorial pyrazolyl arm exchange is detected to 353 K. The activation barrier for pyrazolyl site exchange in **2b** must therefore be greater than 18.4 kcal mol^{-1}. The coupling patterns observed for the respective ethylene ligands in ^{1}H NMR spectra are characteristic of static AA′BB′XY or AA′BB′X spin systems (X = ^{31}P and Y = ^{103}Rh) centered at 1.68 and 0.96 ppm, respectively. No significant change in these patterns is observed from 193 to 353 K. Computer simulations of the complex ethylene multiplets provide the chemical shift and coupling parameters summarized in Table 1. Similar analyses have been reported for related cyclopentadienyl complexes.[22,23] The coupling constants for the ethylene ligand of **2b** are only slightly reduced from those

(16) Fernandez, M. J.; Rodriguez, M. J.; Oro, L. A. *Polyhedron* **1991**, *10*, 1595−1598.
(17) Collman, J. P.; Hegedus, L. S.; Norton, J. R.; Finke, R. G. *Principles and Application of Organotransition Metal Chemistry*; University Science Books: Mill Valley, CA, 1987.
(18) Crabtree, R. H. *The Organometallic Chemistry of the Transition Metals*, 2nd ed.; Wiley: New York, 1994.
(19) Pérez, P. J.; Poveda, M. L.; Carmona, E. *Angew. Chem., Int. Ed. Engl.* **1995**, *34*, 231−233.
(20) Paneque, M.; Poveda, M. L.; Rey, L.; Taboada, S.; Carmona, E.; Ruiz, C. *J. Organomet. Chem.* **1995**, *504*, 147−149.
(21) Shanan-Atidi, H.; Bar-Eli, K. H. *J. Phys. Chem.* **1970**, *74*, 961−963.
(22) Cramer, R.; Kline, J. B.; Roberts, J. D. *J. Am. Chem. Soc.* **1969**, *91*, 2519−2524.
(23) Szajek, L. P.; Lawson, R. J.; Shapley, J. R. *Organometallics* **1991**, *10*, 357−361.

Table 1. ^{1}H NMR Chemical Shift and Coupling Parameters for Coordinated Ethylene in TpM(PPh$_3$)(C$_2$H$_4$) Complexes

	Chemical Shift (ppm)		Coupling Constants (Hz)							
Compound	$\delta_{AA'}$(1, 2)	$\delta_{BB'}$ (3, 4)	J_{12}	J_{34}	J_{13}	J_{14}	J_{15}[a]	J_{35}[a]	J_{16}[b]	J_{36}[b]
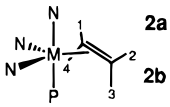 **2a**	1.98[c]	1.38[c]	8.8	8.8	12.1	-3.5	1.2	5.8	2.8	2.6
2b	1.06[d]	0.85[d]	8.8	8.6	8.8	-4.5	1.2	4.5	—	—
Ethylene[e]	5.4		11.6		19.1	2.5				

[a]Phosphorus-hydrogen coupling. [b]Rhodium-hydrogen coupling. [c]THF-d_8. [d]CD_2Cl_2.
[e]Values from Sheppard, N.; Lynden-Bell, R. M. *Proc. Roy. Soc. (London)* **1962**, *A269*, 385-403.

calculated for **1b** (see Experimental Section). Results from selective ^{1}H NMR NOE experiments confirm that the ethylene ligand of **2** occupies an equatorial position of the tbp geometry. Irradiation of the AA′ resonance (1.98 (Rh) or 1.06 (Ir) ppm) of the ethylene ligand gives a strong NOE enhancement of H^3 of the axial pyrazolyl arm and of the BB′ (1.38 (Rh) or 0.85 (Ir) ppm) ethylene resonance. Irradiation of the BB′ resonance gives an NOE enhancement of the AA′ resonance exclusively. Since only a single resonance at high field is observed for the respective ethylene ligands in the ^{13}C{^{1}H} NMR spectra, the ethylene ligand must lie in the equatorial plane with a mirror plane bisecting C=C. The ^{13}C{^{1}H} NMR chemical shifts of the ethylene ligand in **2a**,**b** are shifted significantly upfield to 26.0 and 2.0 ppm, respectively. A similar value of 4.1 ppm has been reported for CpIr(PMe$_3$)(C$_2$H$_4$).[24] The chemical shift of free ethylene, for comparison, is *ca.* 123 ppm. Oro and co-workers have also assigned a tbp structure to TpIr(CO)-(C$_2$H$_4$). ^{1}H NMR NOE experiments verify that the CO and C$_2$H$_4$ ligands occupy axial and equatorial sites, respectively. The lower limit for ethylene rotation in **2** was calculated by computer simulation of the experimental spectra to be greater than 19.8 (**2a**) and 20.8 (**2b**) kcal mol^{-1}. The general observation of hindered ethylene rotation in d^8-ML$_4$(C$_2$H$_4$) complexes arises from the large decrease in metal(π) to C$_2$H$_4$(π*) back-bonding when C$_2$H$_4$ is rotated 90° out of the trigonal plane.[25−27] In our case the facially constrained Tp ligand also prevents Berry-pseudorotation-coupled ethylene rotation.[25] Eisenstein, Caulton, and co-workers have postulated that apical CO ligands should decrease the ethylene rotational barrier by overlap of CO(π*) and C$_2$H$_4$(π*) in the transition state.[28] However, the ethylene ligand of TpIr(CO)(C$_2$H$_4$) has also been reported to be static on the NMR time scale to 373 K,[8] which suggests that the ethylene rotational barriers of **2** are significantly greater than 20 kcal mol^{-1}.

Reactions with Hydrogen. Solutions of **2a** or **2b** react with 1−2 atm of hydrogen to yield TpM(PPh$_3$)H$_2$ (**3a**,**b**) (eq 3). Reactions carried out in sealed NMR tubes

$$\underset{\textbf{2a, b}}{\text{TpM(PPh}_3\text{)(C}_2\text{H}_4\text{)}} \xrightarrow[-\ \text{C}_2\text{H}_4]{+\ \text{H}_2} \underset{\textbf{3a, b}}{\text{TpM(PPh}_3\text{)H}_2} \qquad (3)$$

and monitored by ^{1}H NMR spectroscopy indicate quantitative conversion to **3a**,**b** with displacement of ethylene. When the reactions were carried out with D$_2$, the corresponding dideuteride complexes were formed; however, no deuterium incorporation was observed in the evolved ethylene. Even after complete conversion to **3**, no ethane was observed by ^{1}H NMR analysis. The rates of these reactions as a function of metal center were found to be essentially identical in THF-d_8 ($t_{1/2}$ = *ca.* 30 min). **3** is conveniently prepared in one pot by sequentially reacting **1** with phosphine and then repressurizing a degassed solution with 1−2 atm of H$_2$. Pale yellow (**3a**) or colorless (**3b**) microcrystals are obtained upon addition of pentane to concentrated benzene or toluene solutions. A similar ethylene displacement reaction has been identified for reaction of Pt(PR$_3$)$_2$(C$_2$H$_4$) (R = Me, or Et) with H$_2$.[29] The hydride ligands of **3a**,**b** are identified in solution by ^{1}H NMR (CD_2Cl_2) spectroscopy by their characteristic upfield shifts at −16.42 (dd, J_{P-H} = 28.4 Hz, J_{Rh-H} = 18.9 Hz) and −20.47 ppm (d, J_{P-H} = 22.1 Hz), respectively. IR data for these complexes obtained as Nujol mulls show two M−H bands each at 2092, 2069 cm^{-1} (**3a**) and 2179, 2139 cm^{-1} (**3b**). Appropriate resonances for the Tp and PPh$_3$ ligands were observed in the ^{1}H and ^{13}C{^{1}H} NMR spectra. Interestingly, the protons of the pyrazolyl arm positioned trans to the phosphine ligand weakly couple to the phosphorus nucleus (J_{P-H} = *ca.* 1−2 Hz). ^{1}H{^{31}P} NMR experiments confirm that the origin of the small coupling results from the *trans*-PPh$_3$ ligand. The effect is most pronounced at the H^4-pyrazolyl position, which is five bonds removed from the phosphorus atom and is general for the TpM(PR$_3$) fragment. A number of Tp complexes are known which also contain phosphine donor ligands; however, long-range P−H coupling to the pyrazolyl protons has not been previously reported.

Determination of the Rate Law for Reaction of 2b with H$_2$. The rate law for reaction of **2b** with H$_2$ was determined under pseudo-first-order conditions at

(24) Bell, T. W.; Huddleton, D. M.; McCamley, A.; Partridge, M. G.; Perutz, R. N.; Willner, H. *J. Am. Chem. Soc.* **1990**, *112*, 9212−9226.
(25) Albright, T. A.; Hoffmann, R.; Thibeault, J. C.; Thorn, D. L. *J. Am. Chem. Soc.* **1979**, *101*, 3801−3812.
(26) Rossi, A. R.; Hoffmann, R. *Inorg. Chem.* **1975**, *14*, 365−374.
(27) Segal, J. A.; Johnson, B. F. G. *J. Chem. Soc., Dalton Trans.* **1975**, 677−681.
(28) Lundquist, E. G.; Folting, K.; Streib, W. E.; Huffman, J. C.; Eisenstein, O.; Caulton, K. G. *J. Am. Chem. Soc.* **1990**, *112*, 855−863.
(29) Paonessa, R. S.; Trogler, W. C. *J. Am. Chem. Soc.* **1982**, *104*, 1138−1140.

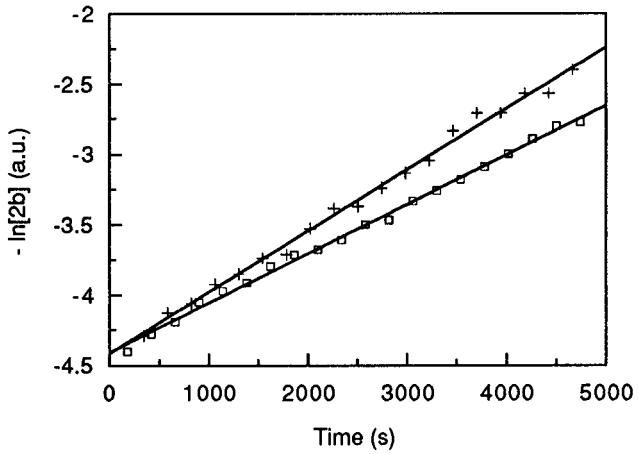

Figure 1. Plot of $-\ln$[**2b**] vs time for reaction of **2b** with H_2 (+) and D_2 (□) in CD_2Cl_2 at 296 K. Conditions: $[\mathbf{2b}]_i = 3.51 \times 10^{-3}$ M; $P_{H_2} = P_{D_2} = 750$ Torr; $[H_2] = 2.3 \times 10^{-3}$ M ($k_{obs}(H_2) = 4.4 \times 10^{-4}$ s^{-1}; $k_{obs}(D_2) = 3.5 \times 10^{-4}$ s^{-1}; $k_H/k_D = 1.26 \pm 0.18$).

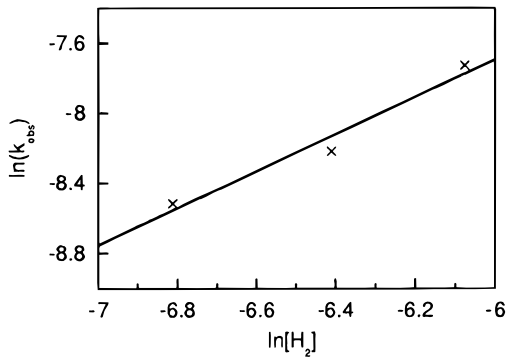

Figure 2. Plot of $\ln(k_{obs})$ vs $\ln[H_2]$ ($r^2 = 0.98$) for the reaction of **2b** with H_2 in CD_2Cl_2 at 296 K. The slope of the line (order in $[H_2]$) is 1.1 ± 0.2.

constant H_2 concentration in the dark. Dilute CD_2Cl_2 solutions of **2b** react cleanly with H_2 to form **3b** and ethylene. A first-order plot of $-\ln$[**2b**] vs time is nicely linear through 3 half-lives (Figure 1). A small isotope effect was observed when the reaction was carried out with D_2 ($k_{H_2}/k_{D_2} = 1.26 \pm 0.18$). Variation of the H_2 pressure from 359 to 750 Torr demonstrates a first-order dependence on $[H_2]$ (Figure 2). No apparent effect on the rate of this reaction was observed when an excess of ethylene was added to the reaction mixture. A slight acceleration was noted when the reaction was run with a 10-fold excess of PPh_3. A side reaction between **2b** and PPh_3 accounts for this observation.[30] These results, summarized in Table 2, indicate an associative rate law for reaction of H_2 with **2b** (eq 4). The observed rate constant (k_{obs}) under pseudo-first-order conditions is equal to $k''[H_2]$, where k'' is the second-order rate constant.

$$\text{rate} = k''[H_2][\mathbf{2b}] \qquad (4)$$

Discussion

As part of our work in the study of hydride structure and dynamics, we required a convenient method to prepare $TpM(PR_3)H_2$ (M = Rh, Ir) complexes.[31] The synthetic methods outlined in this paper provide these species in excellent yield in only three steps from the noble metal salts (eqs 5 and 6). Preliminary results

$$RhCl_3 \cdot 3(H_2O) \longrightarrow [Rh(C_2H_4)_2Cl]_2 \longrightarrow TpRh(C_2H_4)_2 \longrightarrow TpRh(PR_3)H_2 \qquad (5)$$

$$(NH_4)_2IrCl_6 \longrightarrow [Ir(COE)_2Cl]_2 \longrightarrow TpIr(C_2H_4)_2 \longrightarrow TpIr(PR_3)H_2 \qquad (6)$$

indicate that this synthetic method is general for a range of phosphine ligands, including bulky phosphines such as PCy_3 (see Experimental Section). Previous syntheses of complexes related to **3** have been reported;[31−34] however, these procedures are much less convenient and are unlikely to become of general use. The ease with which reactions 2 and 3 occur are in marked contrast to the analogous reactions of the cyclopentadienyl systems. Thermal substitution of ethylene by phosphine ligands occurs only with difficulty,[35−37] if at all,[38] in $(C_5R_5)M(C_2H_4)_2$ (R = H, Me; M = Rh, Ir) complexes. Thermal reactions of $(C_5R_5)M(PR_3)(C_2H_4)$ complexes with H_2 are unknown, as far as we are aware. The difference in reactivity lies in the facile interconversion between 18-electron tbp and 16-electron sp structures in the Tp system. Solution-state structure and dynamics and kinetic data are discussed in the following sections to clarify the proposed reaction mechanisms.

Table 2. Rate Data for the Reaction of 2b with H_2 in CD_2Cl_2 at 296 K[a]

$10^3[\mathbf{2b}]_i$ (M)	$10^3[H_2]$ (M)	10^3[other] (M)	$10^4 k_{obs}$ (s^{-1})
3.51	2.3		4.4
3.51	1.6		2.7
3.51	1.1		2.0
3.51	2.3	35 (C_2H_4)	4.1
3.51	2.3	36 (PPh_3)	5.3
3.51	2.3 (D_2)		3.5

[a] See the Experimental Section for details of the procedure and estimated uncertainties.

Hydridotris(1-pyrazolyl)borate Dynamics. A facile dynamic process serves to exchange the axial and equatorial pyrazolyl ligands of **1** at all accessible temperatures. We have obtained ^{1}H NMR spectra in the fast exchange limit to 130 K in $CDCl_2F$ solutions, indicating an activation energy for this process of less than 6 kcal mol^{-1}. A number of mechanistic studies of Tp fluxionality have concluded that pyrazolyl site exchange occurs within the coordination sphere of the

(30) Heinekey, D. M.; Oldham, W. J., Jr., Wiley, J. S. *J. Am. Chem. Soc.*, **1996**, *118*, 12842−12843.
(31) Heinekey, D. M.; Oldham, W. J., Jr. *J. Am. Chem. Soc.* **1994**, *116*, 3137−3138.
(32) Paneque, M.; Poveda, M. L.; Toboada, S. *J. Am. Chem. Soc.* **1994**, *116*, 4519−4520.
(33) Bovens, M.; Gerfin, T.; Gramlich, V.; Petter, W.; Venanzi, L. M.; Haward, M. T.; Jackson, S. A.; Eisenstein, O. *New J. Chem.* **1992**, *16*, 337−345.
(34) Ferrari, A.; Polo, E.; Rüegger, H.; Sostero, S.; Venanzi, L. M. *Inorg. Chem.* **1996**, *35*, 1602−1608.
(35) Cramer, R. *J. Am. Chem. Soc.* **1972**, *94*, 5681−5685.
(36) Cramer, R.; Seiwell, L. P. *J. Organometal. Chem.* **1975**, *92*, 245−252.
(37) Lawson, R. J. Thesis, University of Illinois, 1978.
(38) Batchelor, R. J.; Einstein, F. W. B.; Lowe, N. D.; Palm, B. A.; Yan, X.; Sutton, D. *Organometallics* **1994**, *13*, 2041−2052.

Scheme 1

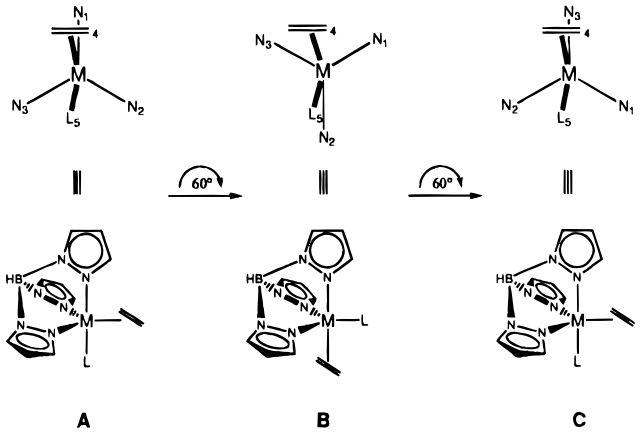

metal, without metal-nitrogen bond cleavage.[4,39−42] Berry pseudorotation (BPR) is commonly proposed to account for dynamic ligand rearrangements in five-coordinate complexes.[43] However, the steric restraints imposed by the bridgehead boron atom prevent the Tp ligand from spanning *trans*-axial sites, which is required for BPR. A more likely mechanism in this case is turnstile rotation (TR).[44] The result of TR is rotation of the Tp ligand around the M···B−H axis by 60°. This mechanism effectively exchanges two axial and equatorial ligands but leaves one of the equatorial ligands unchanged. Considering Scheme 1, conformation **A** depicts axial ligands (N(1) and L(5)) and equatorial ligands, N(2), N(3), and C_2H_4(4). Rotation about the M···B−H axis of 60° produces conformation **B**, with axial sites now occupied by N(2) and C_2H_4(4) and equatorial sites occupied by N(1), N(3), and L(5). Only N(3) remains in a chemically equivalent site following TR. When L(5) is C_2H_4, **A** and **B** are identical. However, when L(5) is any other donor ligand, **B** represents the highest energy intermediate or transition state along the exchange pathway. A second turnstile iteration results in the final structure **C**, in which axial and equatorial pyrazolyl sites have exchanged and the positions of C_2H_4 and L are unchanged from the initial structure **A**. The nature of L has a dramatic effect on the activation barrier of the pyrazolyl exchange process. The activation barriers for the series of complexes TpIr(L)(C_2H_4) (L = C_2H_4, CO,[8] PPh_3) are <6, 14, and >18.4 kcal mol^{-1}, respectively. The barrier of pyrazolyl site exchange for L other than C_2H_4 is a direct measure of the difference in energy between **A** and **B** and increases as the σ-donor ability of L increases. When the metal is changed from Rh to Ir in **2**, the barrier increases by more than 4.1 kcal mol^{-1}.

A second dynamic process, distinct from TR, is equilibrium between tbp and sp structures. It is important to point out that axial and equatorial pyrazolyl arms of a tbp structure are not exchanged by this mechanism. The research groups of Cocivera and Oro have previously demonstrated that equilibria of this type are rapid in complexes that also display rapid TR. Thus, complexes of the type (Bpz_4)M(LL) display only one set of pyrazolyl peaks at ambient temperature. Data reported by Graham and co-workers support the notion that equilibria between sp and tbp structures can also be fast when TR is slow. Both $Tp^{Me2}Rh(CO)(C_2H_4)$ and $Tp^{CF3,Me}Ir(CO)(C_2H_4)$ are assigned sp structures by a systematic comparison of carbonyl stretching bands of related complexes.[5,45] A static sp structure is expected to show a 1:1:1 pattern of pyrazolyl resonances by ^{1}H and ^{13}C NMR analysis. Instead, a 2:1 pattern is observed, which is invariant to −80 °C. A dynamic equilibrium with a tbp intermediate effectively exchanges the uncoordinated pyrazolyl group with only one of the bound ligands (eq 7). TR should be slow in the (η^3-$Tp^{R,R'}$)M(CO)(C_2H_4)

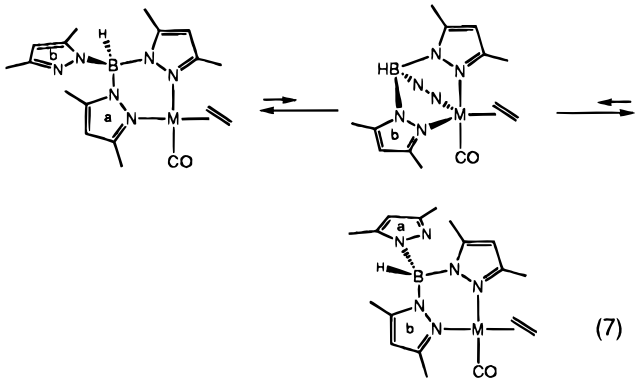

(7)

intermediate for the reasons discussed previously. We propose that a similar equilibrium is obtained for both **1** and **2**, although the tbp form is the more stable isomer. The concentration of the sp form must be very small, because the ^{1}H and ^{13}C NMR chemical shifts show no significant temperature dependence, which might signal a shift in equilibrium concentrations.

Reaction Mechanisms. Complex **1** reacts too rapidly with PPh_3, even at 200 K, to study by conventional NMR methods. In comparison, the reported half-life for reaction of (C_5H_5)M(C_2H_4)$_2$ with excess PPh_3 is 67 (Rh)[35] and 635 min (Ir)[37] at 393 K. These complexes react via high-energy intermediates by either a dissociative or associative mechanism.[36] The latter pathway appears to be more general and may be accommodated if ring slip from η^5- to η^3-C_5H_5 coordination is invoked.[46] We propose that a related process operates in the Tp system. However, in this case 16-electron sp intermediates are close in energy. A reasonable mechanism for reaction of **1** with PPh_3 is outlined in Scheme 2. Nucleophilic attack on the sp intermediate **D** forms the unstable tbp complex **E**. According to a computational study of [Ir(PH_3)$_3$(C_2H_4)$_2$]$^+$, rearrangement to **F** via Berry pseudorotation is at least 30 kcal mol^{-1} downhill.[28] Subsequent displacement of an ethylene ligand by the free pyrazolyl arm yields **2**. An alternative pathway in which an ethylene ligand is displaced directly from **E** is considered less likely because the resulting structure (see **B** in Scheme 1) is known to be particularly unstable.

Solutions of **2** react cleanly with H_2 to give **3** and ethylene. No inhibition of the reaction is observed in

(39) Meakin, P.; Trofimenko, S.; Jesson, J. P. *J. Am. Chem. Soc.* **1972**, *94*, 5677−5681.
(40) Manzer, L. E.; Meakin, P. Z. *Inorg. Chem.* **1976**, *15*, 3117−3120.
(41) Reger, D. L.; Tarquini, M. E. *Inorg. Chem.* **1983**, *22*, 1064−1068.
(42) Steyn, M. M. d. V.; Singleton, E.; Hietkamp, S.; Liles, D. C. *J. Chem. Soc., Dalton Trans.* **1990**, 2991−2997.
(43) Berry, R. S. *J. Chem. Phys.* **1960**, *32*, 933−938.
(44) Ugi, I.; Marquarding, D.; Klusacek, H.; Gillespie, P. *Acc. Chem. Res.* **1971**, *4*, 288−296.
(45) Ghosh, C. K.; Hoyano, J. K.; Krentz, R.; Graham, W. A. G. *J. Am. Chem. Soc.* **1989**, *111*, 5480−5481.
(46) Schuster-Woldan, H. G.; Basolo, F. *J. Am. Chem. Soc.* **1966**, *88*, 1657−1663.

Scheme 2

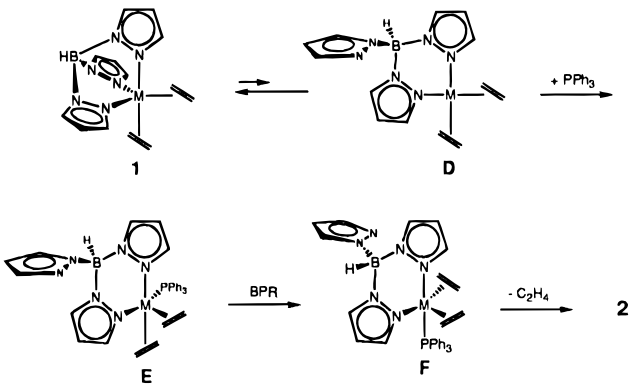

Scheme 3

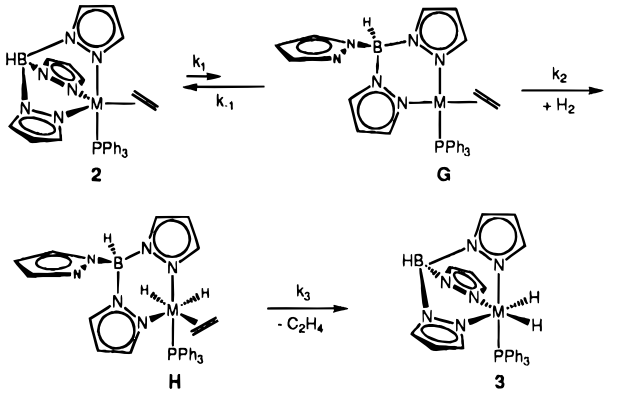

the presence of a large excess of ethylene or PPh_3. Dissociation of these ligands prior to the rate-determining step is thus ruled out. The first-order dependence on $[H_2]$ and the small isotope effect (1.26 ± 0.18) for reactions with D_2 are consistent with oxidative addition of H_2 in the rate-determining step. Oxidative addition of H_2 is well-known in 16-electron sp complexes of rhodium and iridium.[47] A structure of this type is obtained if an equilibrium between tbp and sp structures is invoked for **2**. A mechanism consistent with the experimental observations is outlined in Scheme 3. The rate equation derived for this sequence of steps is shown in eq 8. If we assume that $k_{-1} \gg k_2[H_2]$, then

$$\text{rate} = \frac{k_1 k_2[\mathbf{2b}][H_2]}{k_{-1} + k_2[H_2]} \qquad (8)$$

this equation reduces to the observed rate law (eq 4), where $k'' = k_1k_2/k_{-1}$. This assumption is reasonable because k_1/k_{-1} is small. If H_2 approaches the face opposite the pendant pyrazolyl arm and along the pz−Ir−C_2H_4 axis, the resulting oxidative-addition product **H** is obtained. The ethylene ligand in **H** is positioned trans to the labilizing hydride ligand and is also properly situated for rapid displacement by the pendant pyrazolyl arm. Eisenberg and co-workers have shown that oxidative addition of H_2 to sp iridium complexes occurs stereoselectively along the axis containing a π-acceptor ligand (in this case, ethylene).[48] An interesting test of this rule might be afforded by an examination of the reactions of $TpIr(CO)(C_2H_4)$ or $(H_2B(pz)_2)Ir(CO)(C_2H_4)$ with H_2. Intermediates related to **H** have also been implicated in the reaction of NaTp with $[(NCMe)_3Ir(PMe_3)H_2]SO_3CF_3$. Sequential displacement of the three acetonitrile ligands via $(\eta^1\text{-Tp})Ir(PMe_3)(MeCN)_2H_2$[49] and $(\eta^2\text{-Tp})Ir(PMe_3)(MeCN)H_2$ intermediates ultimately yields $TpIr(PMe_3)H_2$.[31]

Conclusion

The synthesis and characterization of $TpM(PPh_3)(C_2H_4)$ have been described. These complexes provide a convenient entry into hydridotris(pyrazolyl)borate phosphine chemistry of rhodium and iridium. Hydrogen readily displaces the respective ethylene ligands through thermally accessible sp $(\eta^2\text{-Tp})M(PPh_3)(C_2H_4)$ intermediates to form $TpM(PPh_3)H_2$ and free ethylene. The general reactivity of a family of $TpM(PR_3)(C_2H_4)$ complexes is currently under investigation.

Experimental Section

General Methods. All manipulations were conducted under a dry argon or nitrogen atmosphere using standard Schlenk and drybox techniques. Argon and nitrogen were deoxygenated and dried by passage through Chemical Dynamics Corp. R3-11 CuO catalyst followed by Mallinckrodt Aquasorb containing P_2O_5. Air-sensitive compounds were manipulated in an MBraun Labmaster 130 glovebox equipped with integrated Dri-Train loaded with copper catayst and molecular sieves. Solvents were purified by distillation from Na−K−benzophenone (except for CH_2Cl_2, distilled from P_2O_5) under a nitrogen atmosphere. Deuterated NMR solvents (purchased from Cambridge Isotope Laboratories) were degassed and stored over CaH (CD_2Cl_2) or Na−K−benzophenone (C_6D_6, toluene-d_8, THF-d_8). Hydrogen (99.999%) and ethylene (99.7%) were purchased from Airco. Unless stated otherwise, all other reagents were obtained from Aldrich and used as received.

Potassium hydridotris(1-pyrazolyl)borate (KTp) was prepared by the procedure of Trofimenko.[50] $(NH_4)_2IrCl_6$ was recovered from laboratory iridium residues by following published procedures.[51]

^{1}H NMR spectra were recorded on Bruker AC200, AF300, and WM500 spectrometers and referenced internally to the residual proton resonance of the deuterated solvent with respect to tetramethylsilane (TMS). ^{13}C NMR spectra were collected on the AC200, AF300, and WM500 spectrometers operating at frequencies of 50.32, 75.46, and 125.76 MHz, respectively, and referenced internally to the solvent. ^{31}P NMR spectra were collected on the AC200 and WM500 spectrometers at frequencies of 81.02 and 202.45 MHz, respectively, and referenced externally to 85% H_3PO_4. Variable-temperature NMR measurements were performed using the Bruker B-VT1000 temperature control module with a copper−constantan thermocouple. Temperature calibration was obtained by measurement of the chemical shift difference between the $-CH_3$ and $-OH$ peaks of a standard methanol sample using the method of Van Geet.[52] Line-shape analysis of NMR spectra was performed using a modified version of the DYNAMAR program.

(47) James, B. R. *Homogeneous Hydrogenation*; Wiley: New York, 1973.

(48) Johnson, C. E.; Eisenberg, R. *J. Am. Chem. Soc.* **1985**, *107*, 3148−3160.

(49) A monodentate Tp^{t-Bu} complex has recently been structurally characterized: Gutiérrez, E.; Hudson, S. A.; Monge, A.; Nicasio, M. C.; Paneque, M.; Carmona, E. *J. Chem. Soc., Dalton Trans.* **1992**, 2651−2653.

(50) Trofimenko, S. *Inorg. Synth.* **1979**, *12*, 99.

(51) Kauffman, G. B.; Myers, R. D. *Inorg. Synth.* **1978**, *18*, 131−133.

(52) Gordon, A. J.; Ford, R. A. *The Chemist's Companion*; Wiley: New York, 1972; p 303.

Infrared spectra were recorded as Nujol mulls between NaCl plates on a Perkin-Elmer Model 1600 Fourier transform spectrophotometer (2.0 cm^{-1} resolution). Elemental analyses were performed by Canadian Microanalytical Services, Ltd., Vancouver, BC, Canada.

Synthesis of Complexes. TpRh(C_2H_4)$_2$ (1a). This compound was prepared, by following the procedure of Trofimenko,[13] from [Rh(C_2H_4)$_2$Cl]$_2$.[53] Yield: 60%. ^{1}H NMR (C_6D_6; δ): 7.59, 7.41 (d, 3 H each, 3,5-pz); 5.90 (t, 3 H, 4-pz); 2.52 (d, J_{Rh-H} = 1.6 Hz, 8 H, C_2H_4). $^{13}C\{^1H\}$ NMR (C_6D_6; δ): 139.5, 134.8 (s, 3,5-pz); 105.2 (s, 4-pz); 49.0 (d, J_{Rh-C} = 13 Hz, C_2H_4). IR 2461 cm^{-1} (ν_{B-H}).

TpIr(C_2H_4)$_2$ (1b). This compound was prepared, by following the procedure of Tanke and Crabtree,[14] from [Ir(COE)$_2$Cl]$_2$.[54] Yield: 88%. ^{1}H NMR (C_6D_6; δ): 7.64, 7.35 (d, 3 H each, 3,5-pz); 5.80 (t, 3 H, 4-pz); 2.25 (br s, 8 H, C_2H_4). $^{13}C\{^1H\}$ NMR (C_6H_6; δ): 139.4, 134.7 (s, 3,5-pz); 105.6 (s, 4-pz); 29.6 (s, C_2H_4). ^{1}H NMR ($CDCl_2F$, 210 K; δ): 7.81, 7.70 (d, 3 H each, 3,5-pz); 6.25 (t, 3 H, 4-pz); 2.44, 1.70 (m, AA′XX′ spin system, J_{cis} = 9.0, J_{trans} = 11.3, J_{gem} = −2.1 Hz, 2 H each, C_2H_2). IR: 2474 cm^{-1} (ν_{B-H}).

TpRh(PPh$_3$)(C_2H_4) (2a). To a 100 mL Schlenk flask containing TpRh(C_2H_4)$_2$ (0.1124 g, 0.302 mmol), PPh$_3$ (0.0825 g, 0.315 mmol), and a Teflon-coated stirbar was added benzene (10 mL) by cannula. Vigorous bubbling was observed as the solid reagents dissolved, producing a bright yellow solution. This was stirred at room temperature for 60 min, upon which time the volume of the solution was reduced under vacuum and pentane was added to afford a yellow microcrystalline precipitate, which was filtered off and dried under vacuum. Yield: 160 mg (87%). ^{1}H NMR (toluene-d_8; δ): 7.63 (br s, 3 H, 5-pz); 7.40 (br s, 3 H, 3-pz), 7.63−7.18, 6.98 (br m, 15 H, PPh$_3$); 5.82 (t, 3 H, 4-pz); 2.39, 1.77 (m, 2 H each, C_2H_4). ^{1}H NMR (toluene-d_8, 223 K; δ): 7.81 (m, 4 H, *o*-C_6H_5); 7.66 (d, 2 H, 5-pz$_{eq}$); 7.48 (d, 2 H, 3-pz$_{eq}$); 7.44 (br d, 1 H, 5-pz$_{ax}$); 7.12 (br d, 1 H, 3-pz$_{ax}$); 7.03 (m, 6 H, *m*- and *p*-C_6H_5); 6.94, 6.68 (t, J = 8.8 and 7.6 Hz, respectively, 2 H each, *o*- and *m*-C_6H_5); 6.78 (t, J = 6.5 Hz, 1 H, *p*-C_6H_5); 5.83 (t, 2 H, 4-pz$_{eq}$); 5.77 (m, 1 H, 4-pz$_{ax}$); 2.45, 1.83 (m, 2 H each, C_2H_4). ^{1}H NMR (THF-d_8, 219 K; δ): 7.77 (d, 2 H, 5-pz$_{eq}$); 7.70 (br s, 1 H, 5-pz$_{ax}$); 7.62 (m, 4 H, *o*-C_6H_5); 7.48 (m, 6 H, m, *p*-C_6H_5); 7.19 (partially obscurred, 1 H, 3-pz$_{ax}$); 7.18 (d, 2 H, 3-pz$_{eq}$); 7.14 (t, J = 7.4 Hz, 1 H, *p*-C_6H_5); 6.87, 6.68 (t, J = 7.6, 8.6 Hz respectively, 2 H each, *o*- and *m*-C_6H_5); 6.13 (m, 1 H, 4-pz$_{ax}$); 5.92 (t, 2 H, 4-pz$_{eq}$); 1.89, 1.28 (m, 2 H each, C_2H_4). $^{13}C\{^1H\}$ NMR (THF-d_8): 143.8 (s, 3-pz); 135.5 (d, J_{P-C} = 9.8 Hz, *o*- or *m*-PPh$_3$); 134.9 (s, 5-pz); 133.1 (d, J_{P-C} = 45 Hz, *i*-PPh$_3$); 130.5 (s, *p*-PPh$_3$); 128.5 (d, J_{P-C} = 9.6 Hz, *o*- or *m*-PPh$_3$); 104.8 (s, 4-pz); 26.0 (d of d, J_{Rh-C} = 17 Hz, J_{P-C} = 4 Hz, C_2H_4). $^{13}C\{^1H\}$ NMR (THF-d_8, 213 K; δ): 143.8 (s, 3 C, 3-pz$_{ax + eq}$); 135.7 (d, J_{P-C} = 9.8 Hz, 4 C, *o*- or *m*-PPh$_3$); 135.0 (s, 2 C, 5-pz$_{eq}$); 134.9 (s, 1 C, 5-pz$_{ax}$); 132.8 (d, J_{P-C} = 43.5 Hz, 1 C, *i*-PPh$_3$); 132.6 (d, J_{P-C} = 46.5 Hz, 2 C, *i*-PPh$_3$); 130.9 (s, 2 C, *p*-PPh$_3$); 130.2 (s, 1 C, *p*-PPh$_3$); 128.9 (d, J_{P-C} = 9.6 Hz, 4 C, *o*- or *m*-PPh$_3$); 128.1 (d, J_{P-C} = 8.6 Hz, 2 C, *o*- or *m*-PPh$_3$); 105.2 (s, 1 C, 4-pz$_{ax}$); 104.9 (s, 2 C, 4-pz$_{eq}$). $^{31}P\{$aromatic $^1H\}$ NMR (THF-d_8; δ): 57.9 (d of t, J_{Rh-P} = 156 Hz, J_{H-P} = 2.8 Hz). IR: 2468 cm^{-1} (ν_{B-H}). Anal. Calcd for $C_{29}H_{29}BN_6PRh$: C, 57.45; H, 4.82; N, 13.86. Found: C, 56.42; H, 4.67; N, 13.73.

TpIr(PPh$_3$)(C_2H_4) (2b). To a Schlenk flask containing TpIr(C_2H_4)$_2$ (100 mg, 0.22 mmol), PPh$_3$ (61 mg, 0.23 mmol), and a Teflon-coated stirbar was added THF via cannula. The pale yellow solution was stirred at room temperature for 60 min; then the volume was reduced under vacuum. A light yellow precipitate was obtained upon addition of pentane and cooling to −30 °C overnight. This was filtered off, washed with additional pentane, and then dried under vacuum. Yield: 131 mg (86%). ^{1}H NMR (CD_2Cl_2; δ): 7.76, 7.21 (d, 2 H each, 3,5-pz$_{eq}$); 7.69, 7.28 (m and d, respectively, 1 H each, 3,5-pz$_{ax}$); 7.39 (v br, 15 H, PPh$_3$); 6.18 (m, 1 H, 4-pz$_{ax}$); 5.93 (t, 2 H, 4-pz$_{eq}$); 1.07, 0.85 (m, 2 H each, C_2H_4). ^{1}H NMR (CD_2Cl_2, 220 K; δ): 7.76, 7.19 (d, 2 H each, 3,5-pz$_{eq}$); 7.70, 7.23 (br s, 1 H each, 3,5-pz$_{ax}$); 7.51−7.39 (m, 10 H, PPh$_3$); 7.14 (t, J = 7 Hz, 1 H, *p*-C_6H_5); 6.88, 6.58 (t, J = 7 Hz, 2 H each, *o*- and *m*-C_6H_5); 6.18 (m, 1 H, 4-pz$_{ax}$); 5.93 (t, 2 H 4-pz$_{eq}$); 0.95, 0.75 (m, 2 H each, C_2H_4). $^{13}C\{^1H\}$ NMR (CD_2Cl_2; δ): 143.5, 134.9 (s, 2 C each, 3,5-pz$_{eq}$); 135.6, 133.5 (s, 1 C each, 3,5-pz$_{ax}$); 135, 130, 128 (br, PPh$_3$); 105.2 (s, 2 C, 4-pz$_{eq}$); 104.9 (s, 1 C, 4-pz$_{ax}$); 2.0 (s, C_2H_4). $^{31}P\{^1H\}$ NMR (CD_2Cl_2; δ): 9.64 (s). ^{1}H NMR (toluene-d_8; δ): 7.75, 7.00 (extremely broad, 15 H, PPh$_3$); 7.58, 7.42 (d, 2 H each, 3,5-pz$_{eq}$); 7.41, 7.26 (d, 1 H, 3,5-pz$_{ax}$); 5.79 (m, 1 H, 4-pz$_{ax}$); 5.72 (t, 2 H, 4-pz$_{eq}$); 1.59, 1.35 (apparent q and p, respectively, 2 H each, C_2H_4). IR: 2474 cm^{-1} (ν_{B-H}). Anal. Calcd for $C_{29}H_{29}BIrN_6P$: C, 50.08; H, 4.20; N, 12.08. Found: C, 50.71; H, 4.43; N, 11.58.

TpIr(PCy$_3$)(C_2H_4) was prepared as described for **2b**. ^{1}H NMR (C_6D_6; δ): 7.99, 7.67 (d, 2 H each, 3,5-pz$_{eq}$); 7.35, 7.32 (m and d, respectively, 1 H, 3,5-pz$_{ax}$); 6.04 (t, 2 H, 4-pz$_{eq}$); 5.73 (m, 1 H, 4-pz$_{ax}$); 2.55 (p, J = 4 Hz, 2 H, C_2H_4); 1.74 (q, J = 4 Hz, 2 H, C_2H_4); 2.23 (br q, J = 11 Hz, PCy$_3$); 2.5−0.8 (extremely broad envelope of PCy$_3$ resonances). $^{31}P\{^1H\}$ NMR (C_6D_6; δ): −11.04 (s). IR: 2476 cm^{-1} (ν_{B-H}). Anal. Calcd for $C_{29}H_{47}BIrN_6P$: C, 48.81; H, 6.64; N, 11.78. Found: C, 48.19; H, 6.46; N, 11.32.

TpRh(PPh$_3$)H$_2$ (3a). In a 70 mL glass bomb containing TpRh(PPh$_3$)(C_2H_4) (51.9 mg, 0.086 mmol) and a Teflon-coated stirbar was vacuum-transferred benzene (10 mL). The head space was back-filled with hydrogen (1220 Torr) and the flask warmed to room temperature and stirred, protected from light for 16 h. The resulting pale yellow solution was transferred to a Schlenk tube, and the volume was reduced under vacuum. Addition of pentane affords off-white crystals, which were filtered off, washed with pentane, and then dried under vacuum. Yield: 45 mg (91%). A similar procedure, carried out using toluene as solvent and substituting D_2 in place of H_2, provided TpRh(PPh$_3$)D$_2$. ^{1}H NMR (C_6D_6; δ): 7.92, 7.44 (br and m, respectively, 1 H each, 3,5-pz$_{ax}$); 7.69−7.59 (m, 6 H, PPh$_3$); 7.56, 6.78 (d, 2 H each, 3,5-pz$_{eq}$); 6.99−6.93 (m, 9 H, PPh$_3$); 5.84 (m, 1 H, 4-pz$_{ax}$); 5.76 (t, 2 H, 4-pz$_{eq}$); −15.68 (dd, J_{Rh-H} = 18.3 Hz, J_{P-H} = 28.7 Hz, 2 H, Rh−*H*). $^{13}C\{^1H\}$ NMR (C_6D_6; δ): 145.8, 133.8 (s, 1 C, 3,5-pz$_{ax}$); 142.9, 134.5 (s, 2 C, 3,5-pz$_{eq}$); 135.7 (d, J_{P-C} = 48 Hz, *i*-C_6H_5); 134.5 (d, J_{P-C} = 11 Hz, *o*- or *m*-C_6H_5); 129.9 (d, J = 2 Hz, *p*-C_6H_5); 128.2 (partially obscured by C_6D_6, *o*- or *m*-C_6H_5); 105.1 (s, 1 C, 4-pz$_{ax}$); 104.6 (s, 2 C, 4-pz$_{eq}$). $^{31}P\{$aromatic $^1H\}$ NMR (C_6D_6; δ): 63.8 (dt, J_{Rh-P} = 149 Hz, J_{H-P} = 28 Hz). ^{1}H NMR (CD_2Cl_2; δ): 7.70, 7.62 (br s and m, respectively, 1 H each, 3,5-pz$_{ax}$); 7.65, 6.50 (d, 2 H each, 3,5-pz$_{eq}$); 7.44−7.25 (m, 15 H, PPh$_3$); 6.14 (m, 1 H, 4-pz$_{ax}$); 5.88 (t, 2 H, 4-pz$_{eq}$); −16.42 (dd, J_{Rh-H} = 18.9 Hz, J_{P-H} = 28.4 Hz, Rh−*H*). $^{13}C\{^1H\}$ NMR (CD_2Cl_2; δ): 145.7, 135.4 (s, 1 C each, 3,5-pz$_{ax}$); 142.9, 134.8 (s, 2 C each, 3,5-pz$_{eq}$); 135.1 (dd, J_{Rh-C} = 9.8 Hz, J_{P-C} = 47.7 Hz, *i*-C_6H_5); 134.4, 128.4 (d, J_{P-C} = 11 and 10 Hz, respectively, *o*-, *m*-C_6H_5); 130.3 (s, *p*-C_6H_5); 105.3 (s, 1 C, 4-pz$_{ax}$); 104.7 (s, 2 C, 4-pz$_{eq}$). $^{31}P\{$aromatic $^1H\}$ NMR (CD_2Cl_2; δ): 62.3 (dt, J_{Rh-P} = 147 Hz, J_{P-H} = 28 Hz). IR: 2475 (ν_{B-H}); 2092, 2069 (ν_{Rh-H}). Anal. Calcd for $C_{27}H_{27}BN_6PRh$: C, 55.89; H, 4.69; N, 14.48. Found: C, 55.59; H, 4.83; N, 14.12.

TpIr(PPh$_3$)H$_2$ (3b) was prepared in toluene solution by a procedure identical with that employed for the Rh analog. Yield: 95%. ^{1}H NMR (C_6D_6; δ): 8.04, 7.35 (br s and m, respectively, 1 H each, 3,5-pz$_{ax}$); 7.66−7.59 (m, 6 H, PPh$_3$); 7.49, 6.85 (d, 2 H each, 3,5-pz$_{eq}$); 6.99−6.95 (m, 9 H, PPh$_3$); 5.75 (m, 1 H, 4-pz$_{ax}$); 5.67 (t, 2 H, 4-pz$_{eq}$); −19.70 (d, 2 H, J_{P-H} = 23.1 Hz, Ir−*H*). $^{31}P\{$aromatic $^1H\}$ NMR (C_6D_6; δ): 18.8 (t, J_{P-H} = 22.3 Hz). ^{1}H NMR (CD_2Cl_2; δ): 7.83, 7.63 (br s and m, respectively, 1 H each, 3,5-pz$_{ax}$); 7.66, 6.61 (d, 2 H each, 3,5-pz$_{eq}$); 7.39−7.24 (m, 15 H, PPh$_3$); 6.13 (m, 1 H, 4-pz$_{ax}$); 5.86 (t, 2 H, 4-pz$_{eq}$); −20.47 (d, J_{P-H} = 22.1 Hz, 2 H, Ir−*H*). $^{13}C\{^1H\}$ NMR (CD_2Cl_2; δ): 146.4, 134.8 (s, 1 C, 3,5-pz$_{ax}$); 143.3, 134.7 (s, 2 C, 3,5-pz$_{eq}$); 135.3 (d, J_{P-C} = 56 Hz, *i*-C_6H_5); 134.2, 128.2

(53) Cramer, R. *Inorg. Synth.* **1973**, *15*, 14−16.
(54) Onderdelinden, A. L. *Inorg. Synth.* **1974**, *15*, 18.

(d, J_{P-C} = 10 Hz, *o*- and *m*-C_6H_5); 130.1 (s, *p*-C_6H_5); 106.0 (s, 1 C, 4-pz_{ax}); 105.2 (s, 2 C, 4-pz_{eq}). $^{31}P\{$aromatic $^1H\}$ NMR (CD_2Cl_2; δ): 16.9 (t, J_{P-H} = 22.0 Hz). IR: 2481 (ν_{B-H}); 2179, 2139 cm^{-1} (ν_{Ir-H}). Anal. Calcd for $C_{27}H_{27}BIrN_6P$: C, 48.44; H, 4.07; N, 12.55. Found: C, 48.20; H, 4.01; N, 12.24.

Fluxionality. The activation barrier for the exchange of axial and equatorial pyrazolyl ligands in **2a** was determined by monitoring the resonances of 4-pz as a function of temperature. At room temperature a single sharp triplet integrated to three protons is observed at 5.82 ppm. This peak decoalesces at 279 K (300 MHz) into two separate resonances at 5.83 (t, 2 H) and 5.77 ppm (m, 1 H). Using the method of Shanan-Atidi and Bar-Eli[21] for analysis of exchange between unequal populations, an activation energy of exchange was calculated using eq 9, where k_B = Boltzmann's constant, h =

$$\Delta G^{\ddagger} = RT \ln\left[\frac{k_B}{h\pi}\left(\frac{T_c}{\delta_\nu}\right)\left(\frac{X}{1+\Delta P}\right)\right] \qquad (9)$$

Planck's constant, T_c = temperature of coalescence (K), δ_ν = chemical shift difference in the static spectrum (Hz), $X = 2\pi\delta_\nu\tau$ (note $1/\tau = (1/\tau_{eq}) + (1/\tau_{ax})$ when τ_{eq} and τ_{ax} are the lifetimes of the equatorial and axial sites, respectively), and ΔP = difference in mole fractions of the exchanging nuclei. For this problem the ratio of equatorial to axial protons is always 2:1, so that ΔP equals $^1/_3$ (i.e. $^2/_3 - {}^1/_3$). X is evaluated as 2.0823 from Table 6.1 of Sandström's text.[55] The lower limit of pyrazolyl site exhange for **2b** was calculated using the same equation and the limiting chemical shifts at the highest temperature of 353 K.

The lower limit for the barrier to ethylene rotation was calculated using eq 10. The upper limit for the rotational rate

$$\Delta G^{\ddagger} = -RT \ln\left(\frac{kh}{k_B T}\right) \qquad (10)$$

constant (k) used in this equation was determined by simulation of the experimental spectra at the highest temperature of 353 K, using a modified version of the DYNAMAR program. For **2a** and **2b**, k is less than 4 and 1 s^{-1}, respectively.

Kinetic Studies. Kinetic experiments were carried out by monitoring the ^1H NMR spectrum of **2b**/**3b** under H_2 (D_2) in CD_2Cl_2 on a Bruker AF-300 spectrometer. For a given set of experimental conditions a spectrum was acquired every 4 min under computer control for a total of 20 data points (>3 half-lives). Each FID is the sum of 24 scans collected in 60 s (AQ + D1 = 2.5 s). Following data collection, an FID was then written to disk and a delay of 180 s followed, before the next acquisition. The first FID of each data set was Fourier-transformed (FT) and phased. The rest of the files in the data set were then transformed using an AUTOFT routine with the phasing and intensity parameters from the first spectrum. This method allowed an absolute comparison of integral intensities from spectrum to spectrum within one kinetic run. The disappearance of **2b** was followed by monitoring the 4-pz_{eq} resonance at 5.93 ppm. The formation of **3b** was followed by monitoring the 4-pz_{eq} resonance at 5.86 ppm. A standard solution of **2b** (3.51×10^{-3} M) was prepared in the glovebox. Aliquots (0.5 mL) were then transferred to NMR tubes equipped with Kontes valve vacuum line adapters. Using a high-vacuum line, the samples were degassed with three freeze−pump−thaw cycles before adding H_2 (or ethylene). The samples remained frozen in liquid nitrogen during H_2 addition. The pressure of H_2 above the sample was measured using an Omega Series 136 millivolt transducer equipped with an Omega Model DP2000 digital indicator. The Kontes valve was then closed and the tube immersed in liquid nitrogen 1 in. below the point where the sample was flame-sealed. Samples containing ethylene were prepared by first condensing 0.04 mmol of ethylene (calculated from known pressures and volumes) into a frozen, degassed sample at 77 K. H_2 was then added and the tube flame-sealed as described above. A side reaction between **2b** and PPh_3[30] required that samples with PPh_3 be prepared in a slightly different fashion. These were prepared by addition of solid **2b** and PPh_3 (10 equiv) to an NMR tube equipped with a Kontes valve vaccum line adapter. CD_2Cl_2 (0.45 mL) was vaccum-transferred to the NMR tube and the head space back-filled with 750 Torr of H_2. All samples were stored at 77 K until immediately before each kinetic run. The samples were run sequentially by thawing to room temperature (time zero), shaking vigorously for 60 s, and then inserting into the NMR probe. Acquisition of the first FID commenced within 3−5 min of time zero. The concentration of H_2 was measured for a standard CD_2Cl_2 sample under 750 Torr of H_2. The concentration of H_2 at lower pressures was calculated by assuming Henry's law. Integration of the H_2 resonance against a ferrocene standard indicated an H_2 (750 Torr) concentration of 1.7×10^{-3} M. Correction for the fact that 25% of H_2 at room temperature is composed of an NMR-silent spin isomer, i.e. para H_2,[56] gives a true concentration of 2.3×10^{-3} M. The solubility of D_2 was assumed to be identical. This is close to the literature value published for $CHCl_3$ (2.7×10^{-3} M).[57] Pignolet has previously noted that the concentration of H_2 determined by solution NMR methods[58] is significantly smaller than published values.[57,59] ^1H NMR determinations of H_2 concentration will systematically underestimate the true H_2 concentration as a function of the ortho/para H_2 ratio, which is temperature-dependent.[60] Even under the lowest H_2 pressures employed in this study, the total amount of H_2 was at least 20-fold excess. If diffusion of H_2 from the head space into the solution is faster than reaction with **2b**, then pseudo-first-order kinetics are expected. When $[\mathbf{2b}]_i = 3.51 \times 10^{-3}$ M and the H_2 pressure is 750 Torr, these conditions are satisfied (Figure 1). At lower H_2 pressures significant curvature was observed, indicating a diffusion-limited reaction.[61] For these data runs, k_{obs} was calculated from the initial rate using the first four to five data points. The error in k_{obs} is estimated to be ±10% on the basis of the reproducibility of the values.

Acknowledgment. This work was supported by the National Science Foundation. We are grateful for fellowship support (W.J.O.) from the Chevron Research and Technology Co.

OM9605140

(55) Sandström, J. *Dynamic NMR Spectroscopy*; Academic Press: London, 1982.

(56) Abragam, A. *Principles of Nuclear Magnetism*; Oxford University Press: Oxford, U.K., 1983.

(57) *Solubility Data Series: Hydrogen and Deuterium*; Young, C. L., Ed.; Pergamon Press: New York, 1981; Vol. 5/6.

(58) Aubart, M. A.; Chandler, B. D.; Gould, R. A. T.; Krogstad, D. A.; Schoondergang, M. F. J.; Pignolet, L. H. *Inorg. Chem.* **1994**, *33*, 3724−3734.

(59) Fogg, P. G. T.; Gerrand, W. *Solubility of Gases in Liquids*; Wiley: New York, 1991.

(60) An interesting and mechanistically useful consequence of hydrogen spin state isomerism has been recognized by Eisenberg: Eisenberg, R. *Acc. Chem. Res.* **1991**, *24*, 110−116.

(61) Sun, Y.; Landau, R. N.; Wang, J.; Le Blonde, C.; Blackmond, D. G. *J. Am. Chem. Soc.* **1996**, *118*, 1348−1353.